RAD52 aptamer regulates DNA damage repair and STAT3 in BRCA1/BRCA2-deficient human acute myeloid leukemia

YICHUAN XU[1*], YANSI LIN[2*], YUXUAN LUO[3*], YANLING YANG[1], BING LONG[1], ZHIGANG FANG[1], LINGLING LIU[1], JINGWEN ZHANG[1] and XIANGZHONG ZHANG[1]

[1]Department of Hematology, The Third Affiliated Hospital of Sun Yat-sen University, Guangzhou, Guangdong 510630; [2]Department of General Medicine, Sun Yat-sen Memorial Hospital, Sun Yat-sen University, Guangzhou, Guangdong 510120; [3]Department of Pediatrics, Guangzhou Women and Children's Medical Center, Guangzhou, Guangdong 510623, P.R. China

Received November 14, 2019; Accepted July 8, 2020

DOI: 10.3892/or.2020.7723

Abstract. RAD52 (Radiation sensitive 52) is a key factor in DNA damage repair (DDR) bypass, which participates in single-strand annealing (SSA) after DNA damage end excision, while breast cancer type 1 susceptibility protein (BRCA1)/breast cancer type 2 susceptibility protein (BRCA2) play critical roles in homologous recombination (HR) repair. The present study aimed to determine whether RAD52-induced regulation of repair bypass occurs in acute myeloid leukemia (AML) cells and to explore the underlying mechanism. Herein, we applied an RAD52 aptamer to AML cells with downregulated BRCA1/2. RAD52 aptamer inhibited AML cell proliferation detected by cell counting, promoted cell apoptosis obtained by flow cytometry, and suppressed DNA damage repair behavior measured by comet assay and flow cytometry, after drug intervention during low expression of BRCA1/2. During this process, DDR-related cell cycle checkpoint proteins were activated, and the cells were continuously arrested in the S/G2 phase, which affected the cell damage repair process. Concurrently, the expression levels of apoptosis-related proteins were also altered. Furthermore, the expression of STAT3 and p-STAT3 was downregulated by the RAD52 aptamer, suggesting that RAD52 affects the STAT3 signaling pathway. In summary, we present a possible role for RAD52 in DDR of BRCA1/2-deficient AML cells that involves the STAT3 signaling pathway.

Correspondence to: Dr Xiangzhong Zhang or Dr Jingwen Zhang, Department of Hematology, The Third Affiliated Hospital of Sun Yat-sen University, 600 Tianhe Road, Tianhe, Guangzhou, Guangdong 510630, P.R. China
E-mail: zhxzhong@mail.sysu.edu.cn
E-mail: linlin_jw@163.com

*Contributed equally

Key words: RAD52, acute myeloid leukemia, DNA damage repair, apoptosis, STAT3

Introduction

Leukemia is a malignant clonal disease of hematopoietic stem cells (HSCs). During the process of maintaining self-renewal and differentiation, HSCs accumulate a considerable amount of DNA damage under the influence of endogenous or exogenous factors. This damage, either irreparable or only very slowly reparable, leads to genetic mutations, thus causing leukemogenesis (1). At present, the major treatment strategy for leukemia is pharmacotherapy. However, drug resistance, which is exhibited in a considerable number of patients with some mutational genes related to DNA damage repair (DDR) response, has seriously limited its therapeutic effect (2). It is well known that there is a complex but regulatable DDR mechanism *in vivo* that selectively initiates specific repair mechanisms according to different types of DNA damage. For example, DNA suffering from base mismatch or deletion can initiate base excision repair (BER); DNA single-strand breaks (SSBs) can be repaired by specific enzymes *in vivo* such as apurinic/apyrimidinic endonuclease 1 (APE1), polynucleotide kinase 3'-phosphatase (PNKP), and tyrosyl-DNA phosphodiesterase 1 (TDP1); DNA double-strand breaks (DSBs) can initiate the non-homologous end joining repair pathway (NHEJ) or homologous recombination (HR) (3,4).

The single-strand annealing (SSA) repair pathway is a bypass of HR. Unlike the classical pathway, SSA does not depend on the presence of sister chromatids, so the mismatch rate increases significantly (5). RAD52 (Radiation sensitive 52) is a key molecule in the regulation of the SSA process after DNA damage end excision. Previous studies have indicated that the MRN (MRE11/RAD50/NBS1) complex is linked to these breaks, thereby initiating the strand exchange reaction of DNA under the action of RAD52 (6,7). By contrast, accumulating evidence has shown that BRCA1 and BRCA2 are critical components of HR and are downregulated in acute myeloid leukemia (AML) (8,9). Moreover, SSA bypass plays a key role in DDR when HR is incomplete in cells with mutation or downregulation of breast cancer type 1 susceptibility protein (BRCA1)/breast cancer type 2 susceptibility protein (BRCA2) (10). Furthermore, DNA damage-related signaling pathways have been identified by several reports indicating that the downstream cell cycle

checkpoint proteins are activated after DNA damage and thus affect DDR (11,12).

The present study aimed to explore whether RAD52-induced regulation of repair bypass occurs in AML cells and to elucidate the underlying mechanism for this. To this end, we applied an RAD52 aptamer to AML cells with down-regulated BRCA1/2. The effects of the RAD52 aptamer on cell proliferation, cell apoptosis, and DNA damage repair were evaluated after drug intervention. Moreover, expression of apoptosis-related proteins and STAT3 signaling was also detected to explore the underlying mechanism of RAD52 aptamer-induced regulation of AML cells.

Materials and methods

Peptide aptamers. Aptamers are short RNAs or DNAs made up by 20-80 nucleotides. Aptamers can fold into unique three-dimensional conformations to specifically bind to targets (13). F79 synthetic peptide is a member of the aptamers that contains a sequence of 13 amino acids surrounding RAD52 (F79) (VINLANEMFGYNG-GGG-YARAAARQARA), and this was purchased from Genemed Synthesis Inc.. F79 has a three-residue polyglycine linker and protein transduction domain 4; these facilitate passage across lipid bilayers and direct intracellular transduction of the aptamers (14). Aptamers received N-terminal tetramethyl-rhodamine and C-terminal amidation for intracellular detection and reduction of proteolytic degradation (15). F79 aptamers were purified by high-performance liquid chromatography (HPLC) and characterized by mass spectroscopy (MS).

Cell lines and reagents. Human acute myeloid leukemia (AML) cell lines Kasumi-1 and KG1a were obtained from Guangzhou Institute of Biomedicine and Health, Chinese Academy of Sciences, and no mycoplasma infection was confirmed. The STAT3 inhibitor Stattic was purchased from Cayman Chemical Co. (#14590) and was diluted in DMSO. VP16 was purchased from Sigma-Aldrich/Merck KGaA (#E1383) and diluted in DMSO.

Antibodies. CD34 antibody (#555821) and CD38 antibody (#555460) for flow cytometry conjugated with biotin or specific dyes as required were purchased from BD Biosciences; γ-H2AX antibody was purchased from BioLegend (#613402). Western blot-related antibodies were purchased from Cell Signaling Technologies [GAPDH (#2118); BRCA1 (#9010); BRCA2 (#10741); DNA Damage Antibody Sampler Kit, (#9947); H2AX (#2595); CHK2 (#2662); ATM (#2873); ATR (#2790); Bcl2 (#15071) BIM (#2819); STAT3 (#9139); p-STAT3 (#9145)].

Flow cytometry. Cells in logarithmic growth phase were collected at a density of $1x10^6$ per well, washed twice in 2% FBS solution, blocked using Fc (Fc:2% FBS=1:100), and placed on ice for 10-15 min. Antibodies (diluted 1:200) were added, and the cells were incubated for another 15 min in the dark. A blank tube and single stain tubes were set as controls. Fluorescence intensity was detected by BD FACSCalibur (BD Biosciences) and analyzed by FlowJo software (version 7.6; FlowJo, LLC).

Collection of CD34-positive cells. Bone marrow samples were collected from healthy donors, diluted in 2% FBS solution, superimposed on a Ficoll lymphocyte separation solution (#1692254; MP Biomedicals), and gently removed in a single nuclear layer after centrifugation. Cells were resuspended, and red blood cells were lysed on ice for 8-10 min with 3-5 ml of FACS lysing solution (#349202; BD Biosciences). Samples were resuspended in 5-10 ml of 2% FBS and filtered through a 70-μm filter in a 15 ml centrifuge tube. Cells were resuspended in 300 μl MACS buffer (PBS+0.5% BSA+2 mM EDTA), blocked with FcR, and each sample received 100 μl of CD34 magnetic beads (#130-046-702; Miltenyi Biotec, Inc.) in the dark. After incubation for 30 min at 4˚C, the cell suspension was instilled in the column of the magnetic bead separator (#130-042-801; Miltenyi Biotec). The fluid through the magnetic field was discarded, and the remaining cells (CD34-positive) were collected after removal of the magnetic field.

Healthy BM donor samples were collected from i) a 24-year old female, on 2019-8-25, ii) a 40-year-old male, on 2019-8-10, iii) a 38-year-old male, on 2020-9-15, iv) a 29-year-old female, on 2019-9-8, v) a 33-year-old male, on 2019-9-10 and vi) a 28-year-old male, on 2019-9-28.

RT-qPCR. RNA was extracted using a Takara RNA extraction kit (#9767; Shiga, Japan). After the purity and concentration were determined, reverse transcription reaction was performed with the Takara reverse transcription kit, followed by the Takara kit for quantitative polymerase chain reaction. Thermocycling conditions consisted of: Initial denaturation: 95˚C for 30 sec, 39 cycles: 95˚C 5 sec, 60˚C 30 sec, 95˚C for 1 sec, final extension: 65˚C for 5 sec and 95˚C for 5 sec. Data analysis was performed using the $2^{-\Delta\Delta Cq}$ method (16) with GAPDH as the baseline. Primer sequences were as follows: BRCA1 forward, 5'-GGAGGTCAGGAGTTCGAAACC-3' and reverse, 5'-ACCGGCTAATTTCTGTATTTTTAGTAGAG-3'; BRCA2 forward, 5'-ACCTGTTAGTCCCATTTGTACATTTG-3' and reverse, 5'-CACAACTCCTTGGTGGCTGAA-3'; GAPDH forward, 5'-ACCACAGTCCATGCCATCAC-3' and reverse, 5'-TCCACCACCCTGTTGCTGTA-3'.

Drug trials. Cells ($1x10^4$) were seeded into 96-well plates and then treated with 5 μM F79 and different concentrations of VP16 (1, 2, 4, 8, 16 and 32 μg/ml) and incubated at 37˚C in 5% CO_2 for 48 h. The inhibition rate (IR) was evaluated by CCK-8 assay as described below. KG1a and Kasumi-1 cells were treated with 0, 5 μM F79, IC_{50} VP16, 5 μM F79+IC_{50} VP16 at 37˚C in 5% CO_2 for 48 h. Flow cytometry and western blot analysis were conducted by using the cells above. Stattic (0, 2.5, 5, 7.5 and 10 μM) was added to the KG1a cells and incubation was carried at 37˚C in 5% CO_2 for 24 h, and IR was evaluated by CCK-8 assay. γ-H2AX expression level, cell apoptosis rate, cell cycle distribution were measured using flow cytometry between cells treated with 5 μM Stattic and the blank group for 24 h.

Cell proliferation. Different experimental groups were set with triplicate wells each, and cell suspensions were plated in 96-well plates at ~100 μl/well and incubated for 24 h. A 10 μl volume of CCK-8 reagent (#CK04, Dojindo) was added to

each well, plates were incubated for 2 h, and the absorbance at 450 nm was measured. The inhibition rate (IR) was calculated as follows, IR=100%-(Average absorbance of the experimental group-Average absorbance of the blank group)/(Average absorbance of the control group-Average absorbance of the blank group). Data were analyzed by GraphPad Prism software (GraphPad Software, Inc.).

Colony formation assay. Target cells were collected, and methylcellulose (#HSC001; R&D Systems) was added to the cell suspension (1:2), which was completely mixed and seeded in a 24-well plate at ~1 ml/well and cultured in an incubator for 14 days. Cell number >100 was assumed for one colony. The number of colonies was observed and recorded under a microscope (Zeiss Axio Vert. A1; original magnification, x40).

Comet assay. Samples were made according to the Trevigen (#4250-050-K) instruction manual, and the slides were observed under fluorescence microscopy (original magnification, x200).

Western blot analysis. Cells were lysed for 30 min in an ice-cold buffer containing RIPA lysate (~$5x10^5$ cells/ml), PMSF (1:100), leupetin (1:1,000), and $NaVO_3$ (5:1,000). The supernatant was collected, the optical density (OD) value was detected, and the samples were normalized. Samples were electrophoresed at room temperature for 90 min and transferred to a PVDF membrane (ISEQ00010, IPVH00010, Millipore, USA) on ice for 100 min. The required internal reference protein and the target protein bands were blocked at room temperature for 30 min-1 h after excision. Membranes were placed in TBST buffer with the primary antibody (1:2,000 diluted by 5% BSA) overnight at 4˚C followed by the incubation of the secondary antibody (1:5,000 diluted by 5% skim milk, #9947) for 2 h and the addition of ECL solution, with washing between each step. Band densities were observed with ImageJ software (1.51; National Institutes of Health).

Image processing and statistical analysis. Images were processed using Adobe Illustrator (CS6 13.0.0; Adobe Systems Inc.) and GraphPad Prism 6.01 (GraphPad Software, Inc.). All data were analyzed using SPSS Statistics 19 (IBM Corp.) and are presented as mean ± SD. Each experiment was repeated three times. Student's t-tests were performed using statistical software GraphPad Prism v.6, and P-values are indicated in the figure legends. Values are considered significant at $P<0.05$, and the level of significance is noted in the figures as follows: $^{*}P<0.05$ or $^{+}P<0.05$, $^{**}P<0.01$ or $^{++}P<0.01$, $^{***}P<0.001$ or $^{+++}P<0.001$ and $^{****}P<0.0001$ or $^{++++}P<0.0001$.

Results

Expression of BRCA1/BRCA2 is lower in Kasumi-1 and KG1a cells than in primary hematopoietic stem cells. To reflect the response of leukemia stem cells (LSCs) after treatment with chemotherapeutic agents, cell lines with a phenotype close to primary leukemia stem cells were selected for this study. In previous experiments, we found that Kasumi-1 and KG1a cell lines have the highest percentage of CD34-positive cells among the various human acute myeloid leukemia cell lines. Therefore, we examined the ratio of $CD34^+CD38^-$ cells in these two cell lines (Fig. 1A). $CD34^+CD38^-$ cells accounted for 86% of the total Kasumi-1 cells and 93.6% of the total KG1a cells. In addition, normal human bone marrow (BM) samples were collected for sorting $CD34^+$ mononuclear cells, and these were used as the normal hematopoietic stem cell (HSC) control group in subsequent experiments. As shown in Fig. 1B, the percentage of $CD34^+$ cells reached 99% after sorting. In order to better understand the role of BRCA1/2 in DDR, the diagram of related signaling pathways is shown in Fig. 1C. The mRNA and protein expression of BRCA1 and BRCA2 in normal $CD34^+$ HSCs (from BM), Kasumi-1, and KG1a cells was detected by RT-qPCR and western blot analysis (Fig. 1D and E). Expression levels of BRCA1 in Kasumi-1 and KG1a cells were significantly lower than that in the $CD34^+$ HSCs. BRCA2 expression in Kasumi-1 cells was lower than that in the BM HSCs. No statistical difference arose between the mRNA expression levels of BRCA2 in KG1a and $CD34^+$ HSCs, but the expression of BRCA2 protein was significantly lower than that in the $CD34^+$ HSCs. Despite some exceptions, these results indicated that expression of BRCA1/BRCA2 in Kasumi-1 and KG1a cells was lower than that noted in the primary HSCs.

RAD52 aptamer inhibits the cell proliferation of acute myeloid leukemia cells and promotes cell apoptosis. To investigate the effects of the RAD52 aptamer on cell proliferation and apoptosis, human myeloid leukemia cells treated with F79 were subjected to CCK-8 assay to detect the IR of cell proliferation by different concentrations of VP16 and were compared with cancer cells without F79 treatment. As shown in Fig. 2A, treatment with F79 achieved an obviously higher IR of cell proliferation in the VP16-treated Kasumi-1 and KG1a cells. To further explore whether F79 treatment affects cell survival, the cells were divided into a control group (no treatment), F79 group (F79 treatment only), VP16 group (VP16 treatment only), and a combined group (F79+VP16 treatment). No significant difference arose in the apoptotic rate between the F79 group and the control group in Kasumi-1 cells, indicating the ignorable function of mere F79 treatment in cell apoptosis (Fig. 2B). Notably, early apoptosis, late apoptosis, and total apoptotic rate of the combined group were statistically increased compared with those of the VP16 group (Fig. 2B). By contrast, in KG1a cells, no significant difference was found between the F79 group and the control group, while the combined group had an increased early apoptotic rate compared with that of the VP16 group (Fig. 2B). Together, these results clarified that F79 treatment promotes VP16-induced cell apoptosis in human myeloid leukemia cells. In addition, cancer cells were allowed to grow in methylcellulose medium for 14 days to form colonies that were counted at the end of culture. We found that the colony number formed by Kasumi-1 cells in the F79 group was significantly decreased, while no difference between the two groups could be observed in KG1a cells (Fig. 2C). Morphology demonstrated that the colonies formed in the F79 group were generally smaller than those of the control group, and the morphology was uneven (Fig. 2C), indicating that F79 inhibited the growth of the leukemia cells.

Leukemia cells self-repair DNA damage. Intervention of VP16 caused DNA double-strand breaks in LSCs, thus inducing

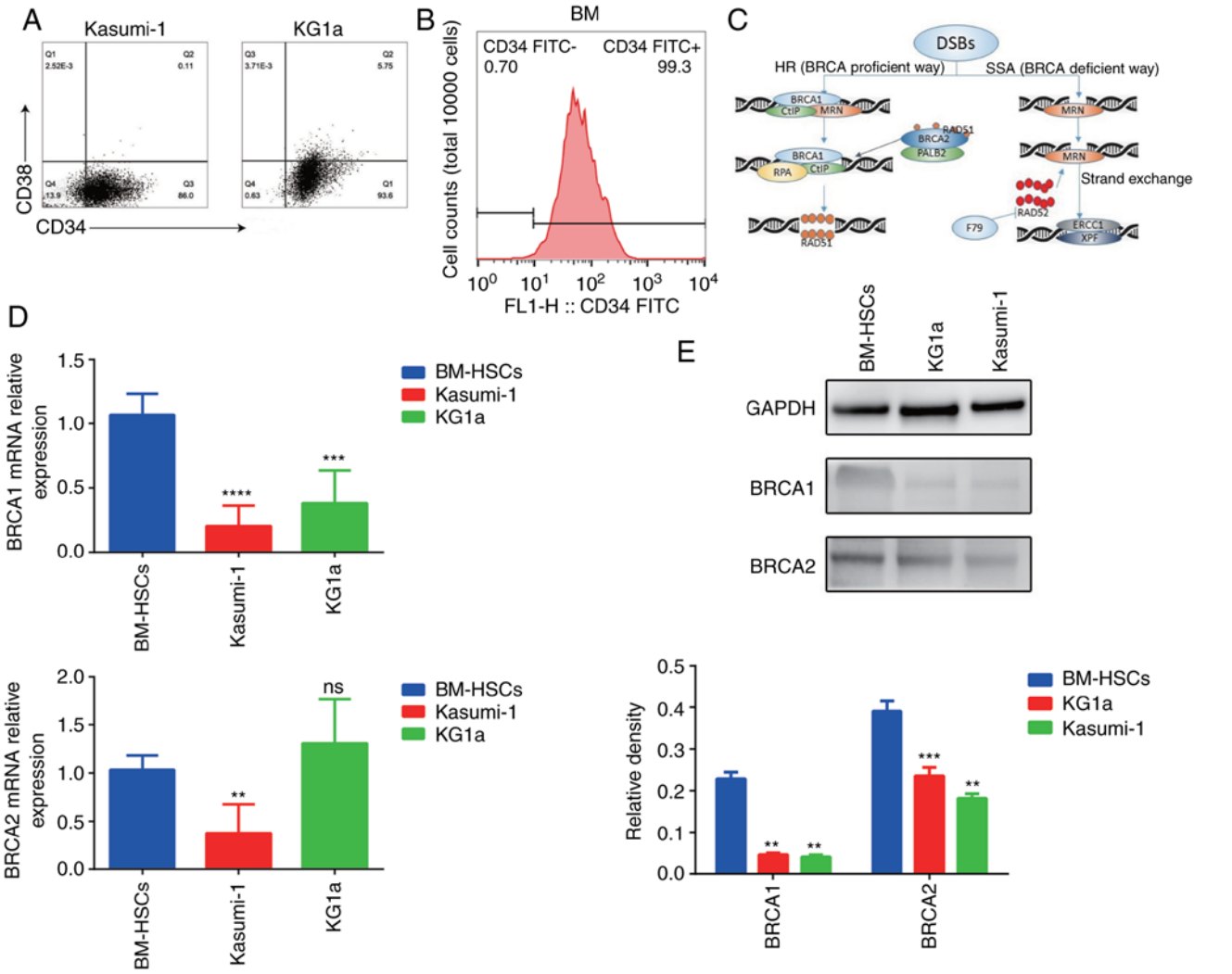

Figure 1. Comparison of BRCA1/BRCA2 mRNA levels in CD34-positive cells of primary and leukemia cell lines. (A) $CD34^+CD38^-$cells accounted for 86% of Kasumi-1 and 93.6% of KG1a cells. (B) $CD34^+$ cells consisted of up to 99% after being sorted from bone marrow of healthy individuals. (C) Diagram of DSB-related signaling pathways. (D) Expression of BRCA1 mRNA in the Kasumi-1 cell line was 0.2040-fold (±0.07139; n=6; bone marrow fluid; ****P<0.0001) of normal BM-HSCs. Expression level of BRCA1 mRNA in the KG1a cell line was 0.3820-fold (±0.1132; n=6; bone marrow fluid; ***P<0.001) of normal BM-HSCs. The expression of BRCA2 mRNA in the Kasumi-1 cell line was 0.3775-fold (±0.1500; n=6; bone marrow fluid; **P<0.01) of normal BM-HSCs. There was no significant difference in the level of BRCA2 mRNA expression in KG1a cell line compared with normal BM-HSCs (bone marrow fluid). (E) Expression of BRCA1 and BRCA2 proteins. The protein expression level of BRCA1 in KG1a and Kasumi-1 was lower than that in the BM-HSCs (n=3; KG1a: **P<0.01; Kasumi-1: **P<0.01). The protein expression level of BRCA2 in KG1a and Kasumi-1 was lower than that in the BM-HSCs (n=3; KG1a: ***P<0.001; Kasumi-1: **P<0.01). BRCA1, breast cancer type 1 susceptibility protein; BRCA2, breast cancer type 2 susceptibility protein; DSB, DNA double-strand breaks; BM-HSCs, bone marrow-hematopoietic stem cells.

serious DNA damage. However, LSCs can repair DNA damage by themselves. In this study, VP16 was utilized for the pretreatment of Kasumi-1 and KG1a cells, and a comet assay and flow cytometry were performed to detect the degree of DNA damage and self-repairing capability after injury. As shown in Fig. 3A, the outcomes of the comet assay exhibited that obvious comet tailing was observed in both Kasumi-1 and KG1a cells after treatment with VP16. In addition, DNA damage repair behavior was observed after 2 h, and no more comet tail was visualized after 4 or 6 h, indicating excellent DNA self-repairing capability. Simultaneously, the mean fluorescence intensity (MFI) of γ-H2AX detected by flow cytometry was significantly increased after drug elution compared with the control group, which decreased gradually in the next 4 h and remained unchanged after that (Fig. 3B). The time variation was roughly consistent with the results of the comet assay, confirming that treatment with VP16 induced DNA damage in Kasumi-1 and KG1a cells, and this was fixed by DNA self-repairing capability.

RAD52 aptamer inhibits DNA damage repair in LSCs. To investigate the effects of the RAD52 aptamer on DNA self-repair capability of LSCs, the cancer cells pretreated with VP16 were subjected to F79 treatment and flow cytometry for detecting MFI of γ-H2AX and were compared with the cells without F79 treatment. Firstly, cells were pretreated with VP16 and divided into a control group and F79 group. After the drug was washed then MFI was detected. As shown in Fig. 4A, although only minor differentiation was observed at 2 and 4 h, the MFI exhibited significant increase at 6 h in the F79 groups of both Kasumi-1 and KG1a cells, indicating that F79 inhibited DNA self-repair. In addition, untreated cells were divided

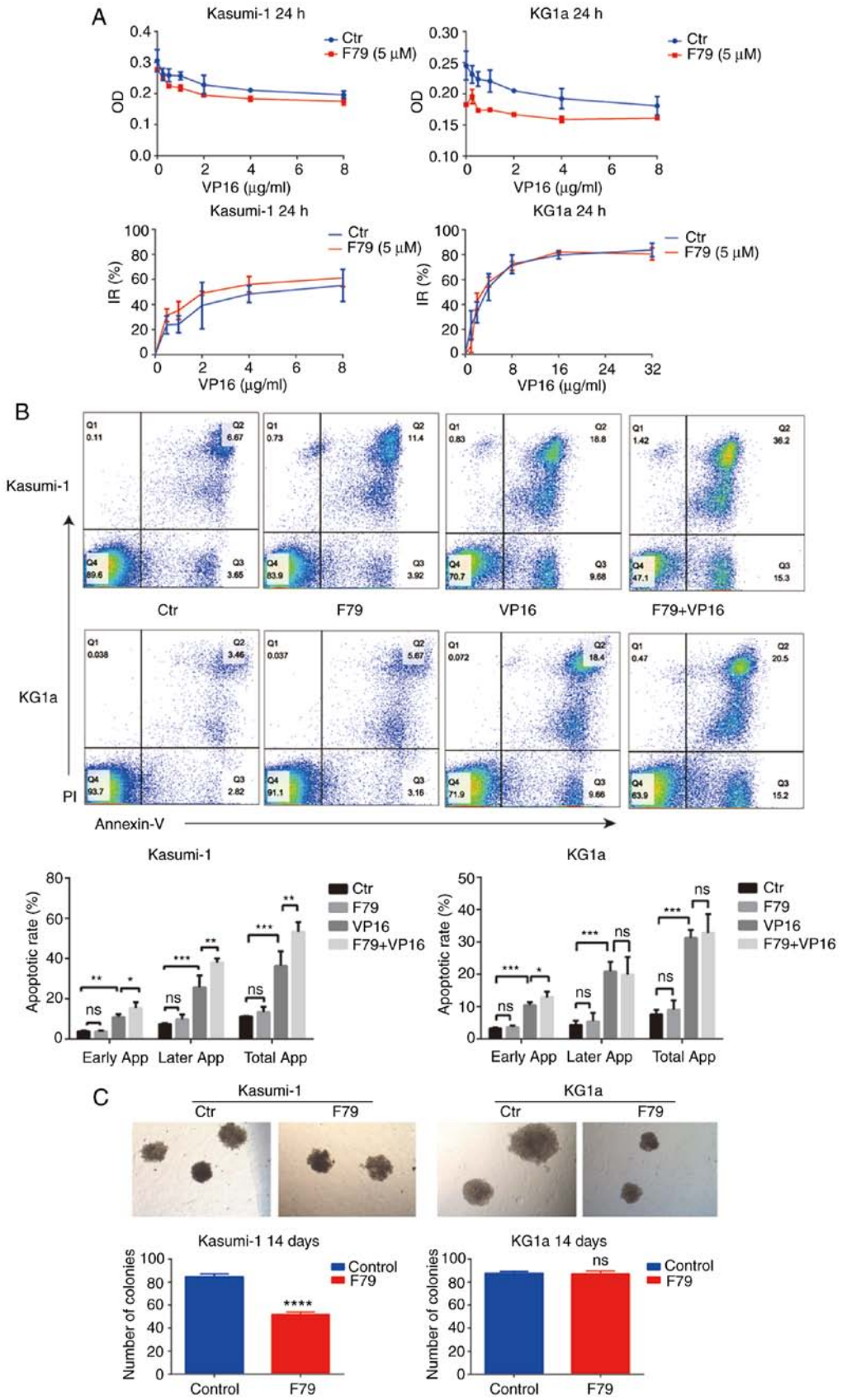

Figure 2. RAD52 aptamer affects the proliferation and apoptosis of leukemia cells. (A) CCK-8 assay was used to detect the optical density (OD) values of the two groups of cells treated with different concentrations of VP16. The OD values of the experimental group were lower than those of the control group. At the same time, the inhibition rate (IR) of cell proliferation was higher in the F79 group than in the control group (n=3). (B) Apoptotic rate of cells from each group was recorded after 48 h of culture. Ctr, blank control group; F79 group, treated with 5 μM F79; VP16 group, treated with IC_{50} concentration of VP16; F79+VP16 group, combination of the two drugs. Data were plotted from triplicate plates. Unpaired Student's t-test (two-tailed) was used for statistical analysis. Data are shown as mean ± SD. *P<0.05, **P<0.01, ***P<0.001; ns, P>0.05, n=3. (C) The number of cell colonies in each group was counted after 14 days of culture. Cell number >100 was assumed for one colony. Kasumi-1: Ctr: n=87, 82, 85; F79: n=50, 52, 54; ****P<0.0001. No colonies were formed in the VP16 group and the combined group. KG1a: Ctr: n=89, 86, 88; F79: n=85, 86, 90; ns, P>0.05. IC_{50}, half maximal inhibitory concentration; VP16, etoposide.

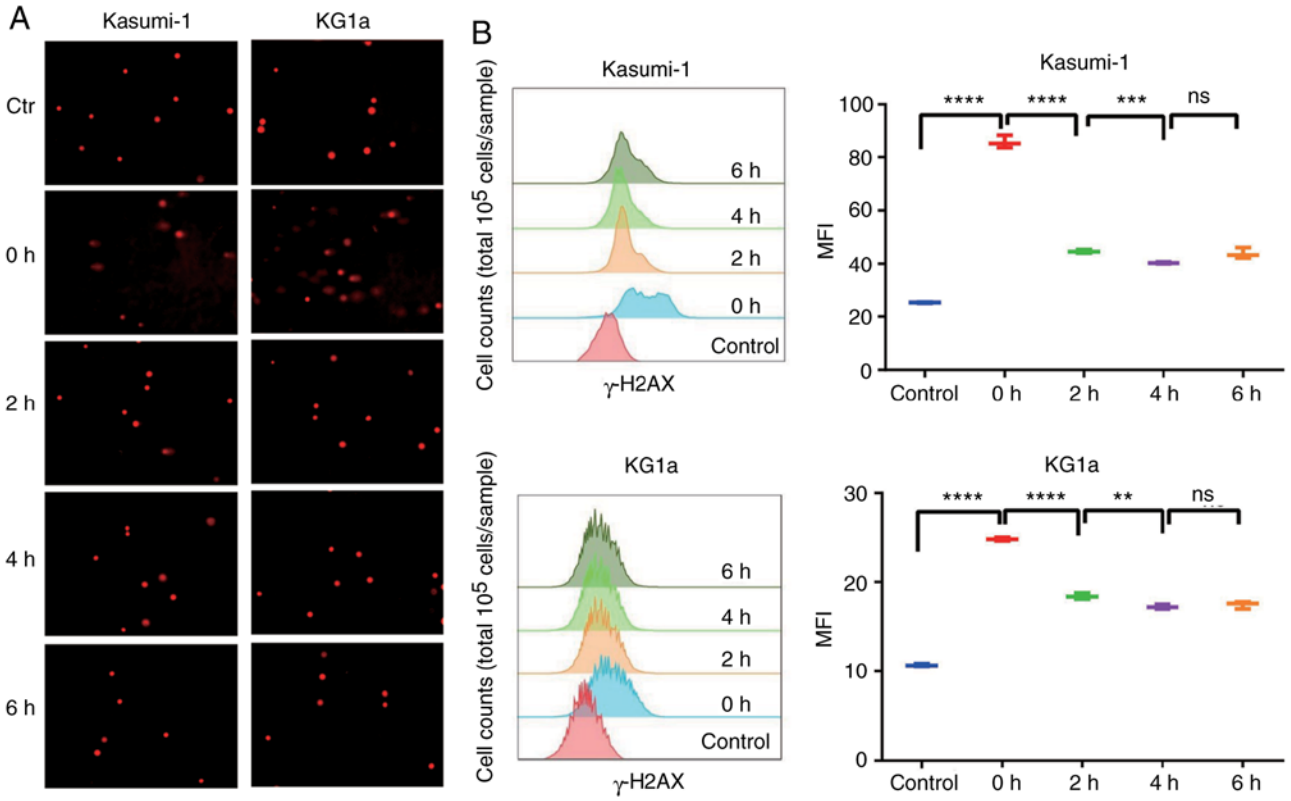

Figure 3. Leukemia cells repair themselves when damaged. (A) Cells were treated with VP16 for 2 h, and the drug was then washed away. Expression of γ-H2AX was detected by comet assay at 0, 2, 4, and 6 h. (B) After treatment of VP16 for 2 h, the expression of γ-H2AX was detected by flow cytometry at 0, 2, 4, and 6 h. The results were expressed as mean fluorescence intensity (MFI); n=3; 0 h, ****P<0.0001 (both cell lines); 2 h, ****P<0.0001 (both cell lines); 4 h, Kasumi-1 ***P<0.001, KG1a **P<0.01. There was no significant difference (ns) at 6 h. VP16, etoposide.

directly into four groups and MFI was detected, respectively. We further verified that F79 increased the MFI of γ-H2AX in cells treated with VP16 at both 2 and 24 h to a much larger extent than that without VP16 treatment (Fig. 4B), indicating the ability of F79 to inhibit the DNA self-repair capability of LSCs with VP16-induced DNA damage.

RAD52 aptamer persistently activates cell cycle-associated checkpoint proteins after suffering DNA damage. Herein, flow cytometry was performed to detect cell cycle distribution of the control group compared with the VP16 group. The proportion of cells both in the S and G2/M phases was significantly increased in the VP16 group compared with control group, suggesting that most of the quiescent cells in the G0/G1 phase entered the cell cycle after VP16 treatment (Fig. 5A). Furthermore, we examined the expression levels of phosphorylated H2AX (p-H2AX), phosphorylated ataxia telangiectasia mutated (p-ATM), phosphorylated ataxia telangiectasia and rad3 related (p-ATR), and phosphorylated checkpoint kinase 2 (p-CHK2). F79 upregulated the expression of p-H2AX (γ-H2AX), p-ATM, p-ATR, and p-CHK2 under the condition of VP16 treatment (Fig. 5B). Collectively, these results confirmed that F79 activated cycle-related checkpoint proteins after the onset of DNA damage, which continuously blocked the cells in the S/G2 phase of the cell cycle, thereby hindering the damage repair process.

Stattic inhibits cell proliferation, promotes cell apoptosis, and affects the process of DDR in AML. We detected the inhibition rate of KG1a cells following treatment with the STAT3 inhibitor Stattic at 1, 2.5, 5, and 10 μM concentration for 24 h. The results suggested that Stattic had an inhibitory effect on KG1a cells in a concentration-dependent manner (Fig. 6A). Flow cytometry was used to detect the apoptosis rate, MFI of γ-H2AX, and the cell cycle distribution. Inhibition of STAT3 by Stattic promoted cell apoptosis (Fig. 6B), which was statistically significant, and increased the MFI of γ-H2AX in the cells (Fig. 6C). In addition, the proportion of cells in the G2/M phase was significantly increased in the Stattic-treated cells (Fig. 6D).

RAD52 aptamer affects the expression of apoptotic signaling pathway proteins. Our previous results showed that F79 increases the apoptotic rate of cells, suggesting that the DNA damage repair pathway may be involved in the activation of the apoptotic signaling pathway. To test this hypothesis, western blot analysis was performed to detect the expression of Bcl2 family members. We found that expression of the anti-apoptotic protein Bcl2 was significantly downregulated upon F79 treatment, while the expression of the pro-apoptotic protein Bim was significantly upregulated (Fig. 7A). Consistent with these and the above experimental results, F79 is thus involved in the activation of the Bcl2-related apoptotic pathway.

Continuous activation of STAT3 is commonly observed in human myeloid leukemia cells. In this context, to explore whether STAT3 participates in the SSA repair pathway, we utilized western blot analysis to detect the protein expression

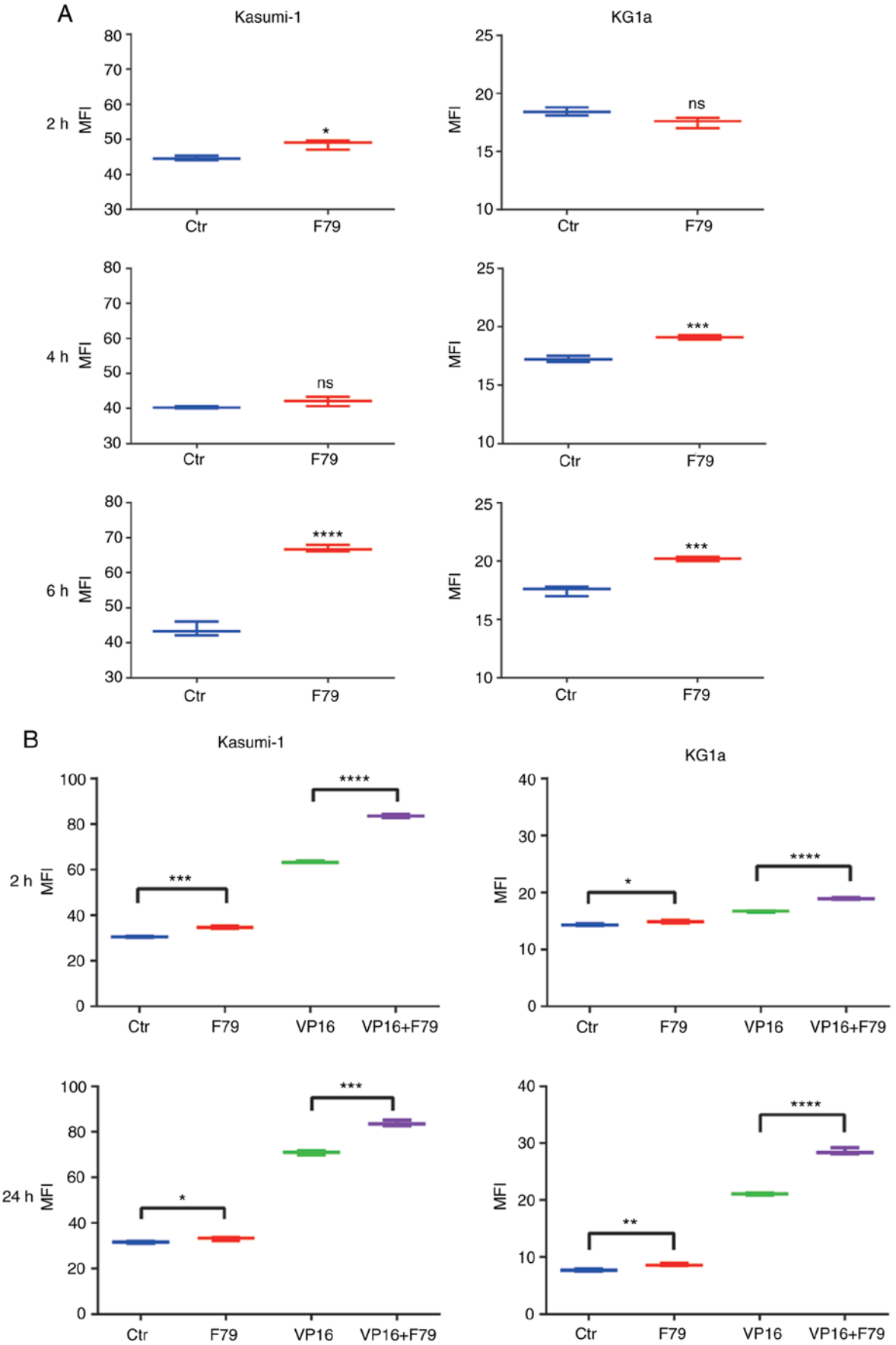

Figure 4. Effect of RAD52 aptamer on DNA damage repair in leukemia cells. (A) Cells were pretreated with VP16 and divided into control group and F79 (5 μM) group. Flow cytometry was used to detect the expression of γ-H2AX at indicated time points, n=3. (B) Detection of mean fluorescence intensity (MFI) in different groups at 2 and 24 h. Ctr, blank control group; F79 group, cells treated with 5 μM F79; VP16 group, cells treated with IC_{50} concentration of VP16; F79+VP16 group, combined treatment of the two drugs; n=3. *P<0.05, **P<0.01, ***P<0.001, ****P<0.0001; ns, P>0.05. IC_{50}, half maximal inhibitory concentration; VP16, etoposide.

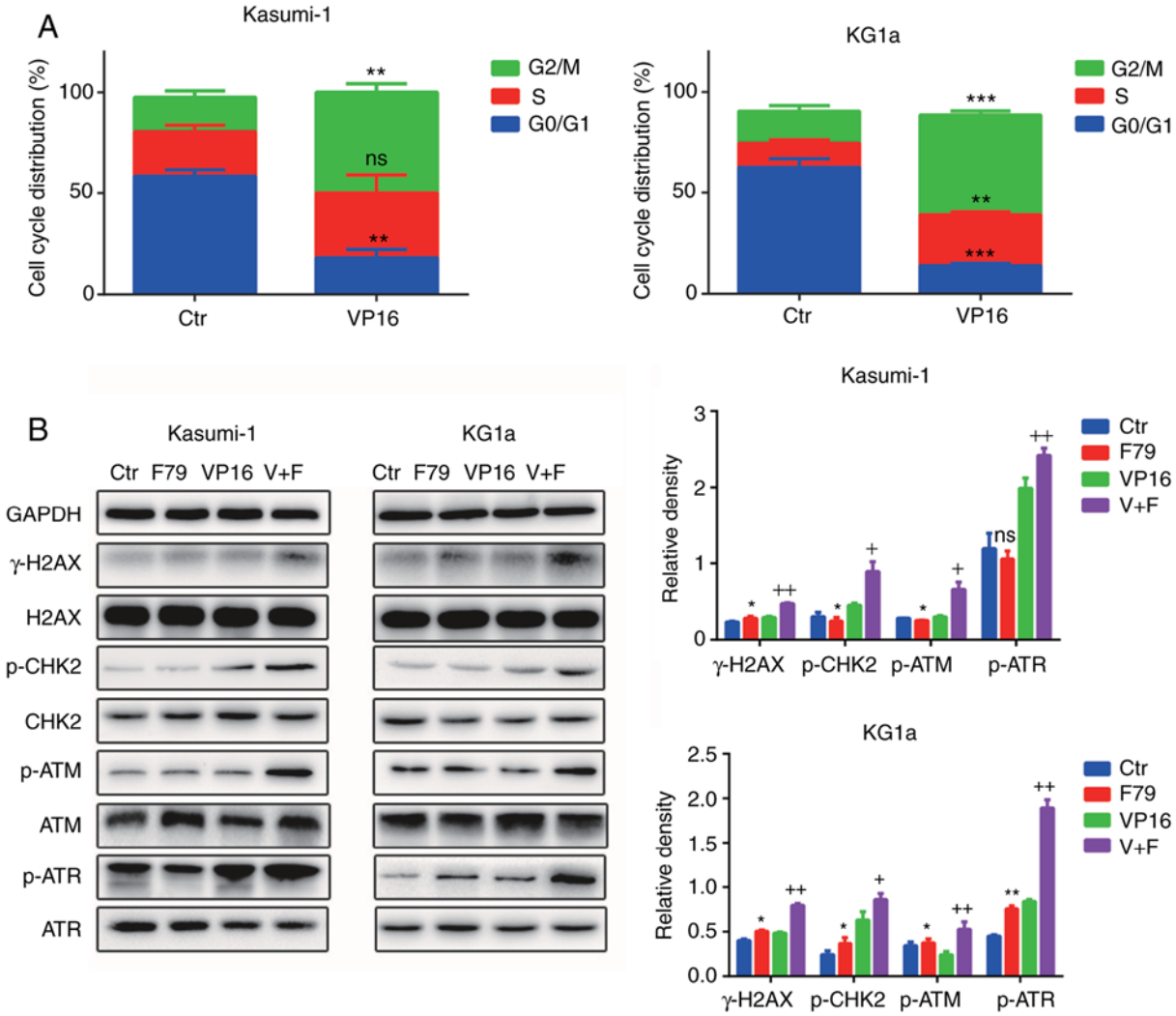

Figure 5. The RAD52 aptamer activates cell-cycle-associated checkpoint protein in damaged cells, allowing cells to persist in the S/G2 phase. (A) Flow cytometry was used to detect the cell cycle distribution before and after treatment with VP16. **P<0.01, ***P<0.001 and ns, P>0.05, compared to the Ctr, n=3. (B) The protein expression of p-H2AX (γ-H2AX), p-ATM, p-ATR and p-CHK2 in cell lines was detected by western blot analysis before and after treatment with VP16. Ctr, blank control group; F79 group, cells treated with 5 μM F79; VP16 group, cells treated with IC_{50} concentration of VP16; V+F group, combined treatment of the two drugs. The results were compared by relative band density (n=3). *P<0.05, F79 group compared with the Ctr group; $^{+}$P<0.05, $^{++}$P<0.01, the combined group (V+F) compared with the VP16 group. p-ATM, phosphorylated ataxia telangiectasia mutated; p-ATR, phosphorylated ataxia telangiectasia and rad3 related; p-CHK2, phosphorylated checkpoint kinase 2; VP16, etoposide.

of STAT3 protein and its activated, phosphorylated form (p-STAT3). The results showed that F79 significantly downregulated the expression of STAT3 and p-STAT3 after VP16-induced DNA damage (Fig. 7B), which indicated that SSA may regulate cell proliferation and apoptosis by affecting the JAK-STAT signaling pathway.

Discussion

In the present study, we verified the activity of the single-strand annealing (SSA) repair bypass wherein RAD52 (Radiation sensitive 52) is involved in affecting the proliferation and apoptosis of leukemia cells under BRCA1/BRCA2 down-regulation and detected the severity of DNA damage before and after VP16 (etoposide) intervention. We found that VP16-induced DNA damage was repaired by the cells themselves in a short time, while treatment of cells with RAD52 aptamer F79 prevented the cells from repairing DNA damage and decreased this DNA self-repairing ability. Some leukemia patients are resistant to chemotherapy drugs as leukemia stem cells (LSCs) *in vivo* own a rapid DNA damage-repair ability, preventing tumor cells from death (17). The homologous recombination (HR) pathway plays a leading role in DNA damage repair (DDR) (18). However, the efficacy of HR is greatly limited in acute myeloid leukemia cells with downregulated BRCA1/BRCA2 expression. The SSA pathway leads to the lethality of cells suffering from severe DNA damage after the HR pathway is injured. Our research further emphasizes that synthetic lethality can be achieved by blocking RAD52 in AML through different experimental methods.

In addition, we found that cell-cycle checkpoint proteins were upregulated during drug intervention. Meanwhile, the expression of anti-apoptotic protein Bcl-2 was downregulated in cells treated with F79, while the expression of pro-apoptotic protein Bim was upregulated. When ataxia telangiectasia mutated (ATM) and ataxia telangiectasia and rad3 related

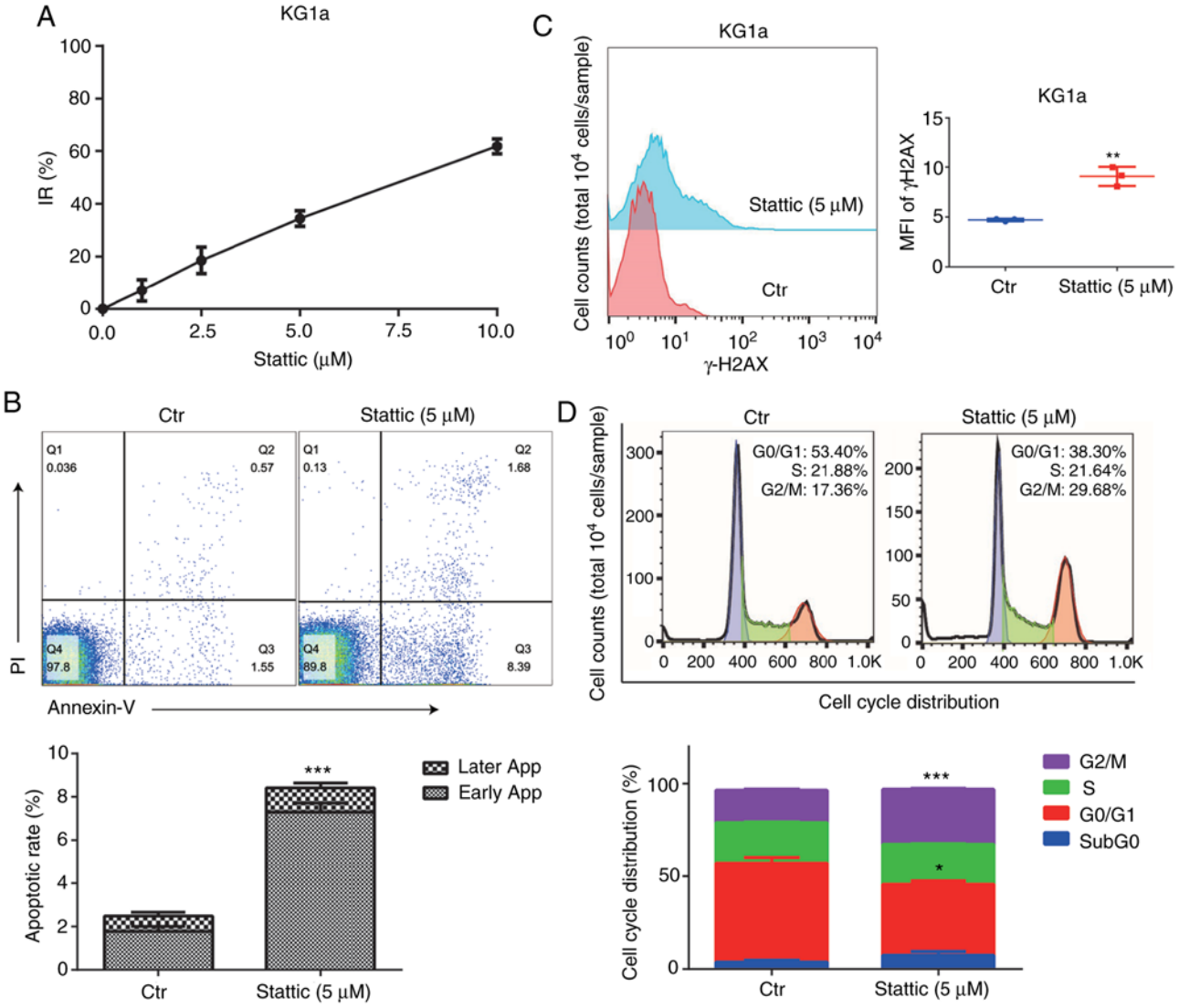

Figure 6. Effect of STAT3 inhibitor Stattic on cell survival and DNA damage repair in AML cells. (A) CCK-8 assay was used to detect the optical density (OD) value of the cells treated with different concentrations of Stattic for 24 h, and the inhibition rate (IR) of cell proliferation was calculated. (B) After treatment of Stattic (5 μM) for 24 h, the apoptotic rate was detected by flow cytometry. ***P<0.001, compared with the Ctr group, n=3. (C) Detection of mean fluorescence intensity (MFI) in both groups: Ctr, blank group; Stattic group (5 μM). **P<0.01, compared with the Ctr group, n=3. (D) Flow cytometry was used to detect the cell cycle distribution before and after treatment with Stattic. *P<0.05, ***P<0.001, compared with the Ctr group, n=3.

(ATR) are recruited to double-strand breaks (DSBs), they phosphorylate themselves and downstream signaling proteins such as p53 and DDR-related cell cycle checkpoint proteins such as checkpoint kinase (CHK)1, CHK2, and CDC25. Activation of checkpoint proteins causes temporary cell-cycle arrest (2,19,20). Once the damage is repaired, the cells can undergo a normal cycle, while continuous cell cycle arrest activates the apoptotic pathway proteins and promotes cell apoptosis. It has been reported that when the cell cycle checkpoint is activated, p53 protein, which is capable of regulating and promoting cell apoptosis by downregulating the expression of Bcl-2, is also activated (3,21,22). Our study indicates that AML cells after F79 intervention were in a state of continuous cell cycle arrest and eventually led to their death. We proposed that the SSA may activate upstream or downstream proteins of the Bcl2-related apoptotic pathway, which in turn affects cell survival and is likely to affect the expression of the p53 protein. However, p53 has been found to be mutated in a variety of tumor cells, and its mutation types are diverse, making it difficult to be accurately targeted (23). Therefore, the presence of another signal transduction pathway associated with DDR under the SSA pathway has yet to be fully reported.

Clinically, we have seen an increase in acute myeloid leukemia (AML) patients with STAT3 activation and found that AML patients with STAT3 activation are prone to drug resistance. Our study showed that inhibition of STAT3 played a role in cell survival and DDR. Furthermore, STAT3 and its activated form (p-STAT3) were downregulated in LSCs treated with RAD52 aptamer, indicating that the SSA pathway may affect the expression of STAT3. STAT3 is often seen activated in leukemia cells (24). However, the continuous activation of STAT3 in myeloid leukemia cells may be related to drug resistance and has become an urgent problem to be solved for killing leukemia cells (25). In recent years, many studies have found that STAT3 is involved in DDR, especially during cell-cycle checkpoint activation, in the cells of other types of malignant

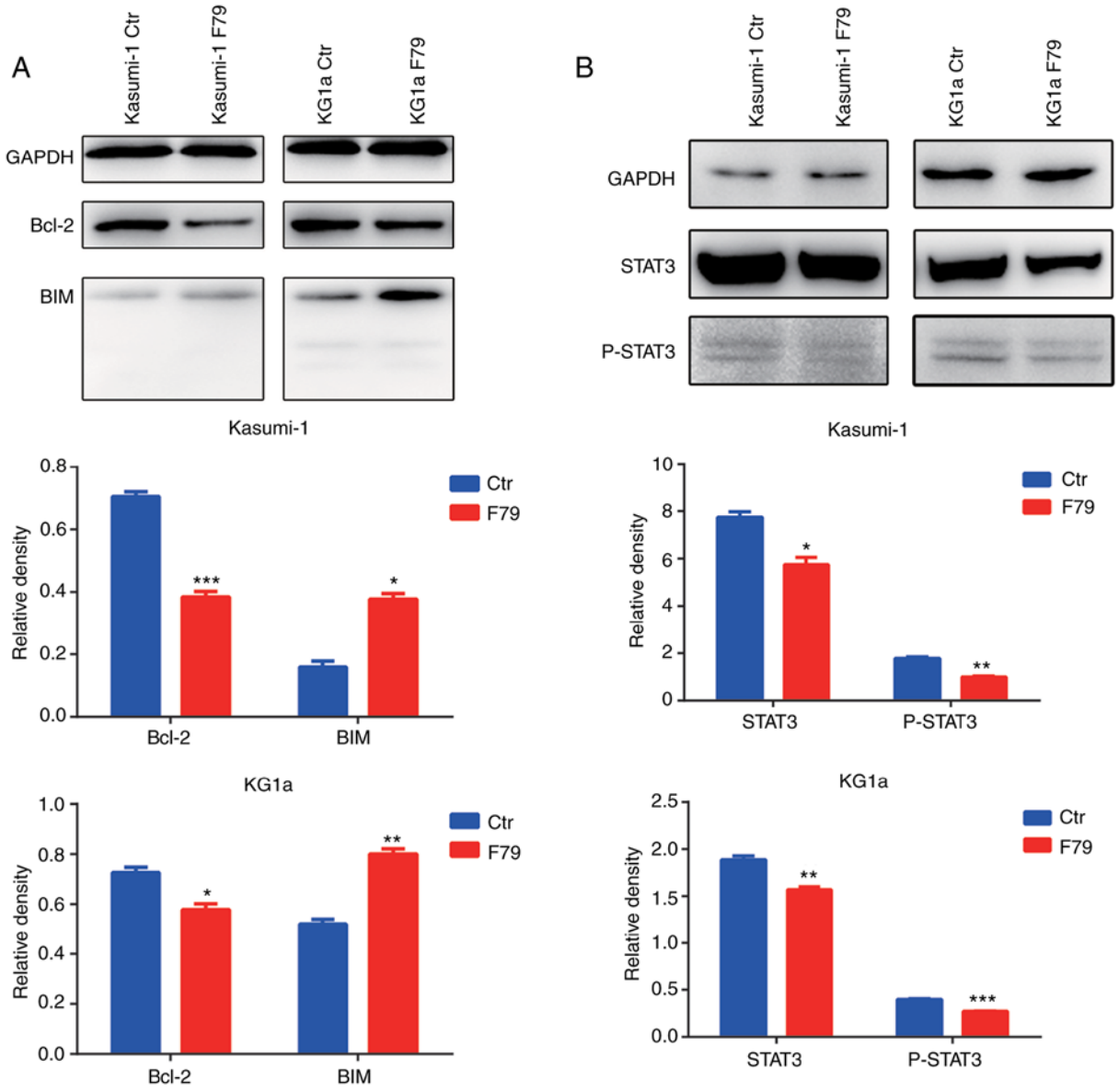

Figure 7. Expression of proteins related to the Bcl2 family and STAT3. (A) The protein expression of Bcl-2 and Bim in cell lines was detected by western blot analysis before and after treatment with F79. The results were compared by relative band density (n=3). (B) The protein expression of STAT3 and p-STAT3 in cell lines was detected by western blot analysis before and after treatment with F79. The results were compared by relative band density (n=3). Ctr, blank control group; F79 group, cells treated with 5 μM F79. *P<0.05, **P<0.01, ***P<0.001, compared with the Ctrl group, n=3. p-STAT3, phosphorylated signal transducer and activator of transcription 3.

tumors (26-29). Reportedly, STAT3 prevents the transmission of the ATR-CHK1 signaling pathway, thereby inhibiting the progression of DDR in S phase (27). However, downregulation of STAT3 inhibits the activation of ATR-CHK1 and ATM-CHK2 signaling, which in turn attenuates the activation of checkpoint proteins in the S/G2 phase (26). Other studies have shown that STAT3 is indeed involved in the regulation of DDR and the downstream apoptosis pathway in cancer cells (30), but how STAT3 works in AML cells has not been reported. Here, we preliminarily demonstrated that the downregulation of STAT3 or p-STAT3 affects DDR, and RAD52 may regulate the STAT3-related signaling pathway. However, the specific mechanism remains unclear.

Our study had several limitations. The experiments used to determine the anti-leukemia mechanism with F79 intervention were limited. We simply focused on the inhibitory effect of DNA repair by RAD52 and no further study was carried out on the concentration-dependent changes after drug intervention. In addition, we found that STAT3 and p-STAT3 were downregulated after F79 treatment, while a similar phenomenon could be induced by the STAT3 inhibitor. However, the evidence of amplifying STAT signaling function in DDR and the relationship with the SSA pathway is insufficient. Further studies are required to verify these hypotheses.

In summary, we demonstrated that RAD52 has a significant role in regulating cell survival and DDR in AML with low expression of BRCA1/BRCA2. After F79 intervention, we found leukemia cells to be in a poor condition of DNA repair, which may be related to the expression of STAT3. Collectively, these data may provide new insights into leukemia drug therapy.

Acknowledgements

Not applicable.

Funding

This work was supported by Basic Research Program from the Guangdong Natural Science Foundation (S2013010016559 and 2014A030313138).

Availability of data and materials

All data generated or analyzed during this study are included in this published article.

Authors' contributions

YX, YaL and YuL designed the study, conducted the experiments and analyzed the data. YY, BL, ZF and LL collected the human samples and were accountable for all aspects of the work in ensuring that questions related to the accuracy or integrity of any part of the work are appropriately investigated and resolved. JZ supervised the study, wrote the manuscript and revised it critically for important intellectual content. XZ put forward ideas for research, reviewed the results and approved the final version of the manuscript. All authors read and approved the manuscript and agree to be accountable for all aspects of the research in ensuring that the accuracy or integrity of any part of the work are appropriately investigated and resolved.

Ethics approval and consent to participate

All procedures performed in studies involving human participants were in accordance with the ethical standards of the National Science and Technology Ethics Committee and with the 1964 Helsinki Declaration and its later amendments or comparable ethical standards. We obtained ethics approval from the Medical Ethics Committee of the Third Affiliated Hospital of Sun Yat-sen University, [(2020)-02-068-01]. All donors signed the informed consent form.

Patient consent for publication

Not applicable.

Competing interests

The authors state that they have no competing interests.

References

1. Moehrle BM and Geiger H: Aging of hematopoietic stem cells: DNA damage and mutations? Exp Hematol 44: 895-901, 2016.
2. Esposito MT and So CW: DNA damage accumulation and repair defects in acute myeloid leukemia: Implications for pathogenesis, disease progression, and chemotherapy resistance. Chromosoma 123: 545-561, 2014.
3. Biechonski S, Yassin M and Milyavsky M: DNA-damage response in hematopoietic stem cells: An evolutionary trade-off between blood regeneration and leukemia suppression. Carcinogenesis 38: 367-377, 2017.
4. Iyama T and Wilson DM III: DNA repair mechanisms in dividing and non-dividing cells. DNA Repair (Amst) 12: 620-636, 2013.
5. Bhargava R, Onyango DO and Stark JM: Regulation of single-strand annealing and its role in genome maintenance. Trends Genet 32: 566-575, 2016.
6. Symington LS: Role of RAD52 epistasis group genes in homologous recombination and double-strand break repair. Microbiol Mol Biol Rev 66: 630-670, table of contents, 2002.
7. Rothenberg E, Grimme JM, Spies M and Ha T: Human Rad52-mediated homology search and annealing occurs by continuous interactions between overlapping nucleoprotein complexes. Proc Natl Acad Sci USA 105: 20274-20279, 2008.
8. Faraoni I, Compagnone M, Lavorgna S, Angelini DF, Cencioni MT, Piras E, Panetta P, Ottone T, Dolci S, Venditti A, *et al*: BRCA1, PARP1 and γH2AX in acute myeloid leukemia: Role as biomarkers of response to the PARP inhibitor olaparib. Biochim Biophys Acta 1852: 462-472, 2015.
9. Scardocci A, Guidi F, D'Alo' F, Gumiero D, Fabiani E, Diruscio A, Martini M, Larocca LM, Zollino M, Hohaus S, *et al*: Reduced BRCA1 expression due to promoter hypermethylation in therapy-related acute myeloid leukaemia. Br J Cancer 95: 1108-1113, 2006.
10. Cramer-Morales K, Nieborowska-Skorska M, Scheibner K, Padget M, Irvine DA, Sliwinski T, Haas K, Lee J, Geng H, Roy D, *et al*: Personalized synthetic lethality induced by targeting RAD52 in leukemias identified by gene mutation and expression profile. Blood 122: 1293-1304, 2013.
11. Panier S and Boulton SJ: Double-strand break repair: 53BP1 comes into focus. Nat Rev Mol Cell Biol 15: 7-18, 2014.
12. van Attikum H and Gasser SM: Crosstalk between histone modifications during the DNA damage response. Trends Cell Biol 19: 207-217, 2009.
13. Guan B and Zhang X: Aptamers as versatile ligands for biomedical and pharmaceutical applications. Int J Nanomedicine 15: 1059-1071, 2020.
14. Borghouts C, Kunz C and Groner B: Current strategies for the development of peptide-based anti-cancer therapeutics. J Pept Sci 11: 713-726, 2005.
15. Slupianek A, Dasgupta Y, Ren SY, Gurdek E, Donlin M, Nieborowska-Skorska M, Fleury F and Skorski T: Targeting RAD51 phosphotyrosine-315 to prevent unfaithful recombination repair in BCR-ABL1 leukemia. Blood 118: 1062-1068, 2011.
16. Livak KJ and Schmittgen TD: Analysis of relative gene expression data using real-time quantitative PCR and the 2(-Delta Delta C(T)) method. Methods 25: 402-408, 2001.
17. Ciccia A and Elledge SJ: The DNA damage response: Making it safe to play with knives. Mol Cell 40: 179-204, 2010.
18. Stadler J and Richly H: Regulation of DNA repair mechanisms: How the chromatin environment regulates the DNA damage response. Int J Mol Sci 18: 1715, 2017.
19. Gaul L, Mandl-Weber S, Baumann P, Emmerich B and Schmidmaier R: Bendamustine induces G2 cell cycle arrest and apoptosis in myeloma cells: The role of ATM-Chk2-Cdc25A and ATM-p53-p21-pathways. J Cancer Res Clin Oncol 134: 245-253, 2008.
20. Xiao Z, Chen Z, Gunasekera AH, Sowin TJ, Rosenberg SH, Fesik S and Zhang H: Chk1 mediates S and G2 arrests through Cdc25A degradation in response to DNA-damaging agents. J Biol Chem 278: 21767-21773, 2003.
21. Rivlin N, Koifman G and Rotter V: p53 orchestrates between normal differentiation and cancer. Semin Cancer Biol 32: 10-17, 2015.
22. Vousden KH and Prives C: Blinded by the light: The growing complexity of p53. Cell 137: 413-431, 2009.
23. Bykov VJN, Eriksson SE, Bianchi J and Wiman KG: Targeting mutant p53 for efficient cancer therapy. Nat Rev Cancer 18: 89-102, 2018.
24. Bruserud Ø, Nepstad I, Hauge M, Hatfield KJ and Reikvam H: STAT3 as a possible therapeutic target in human malignancies: Lessons from acute myeloid leukemia. Expert Rev Hematol 8: 29-41, 2015.
25. Al Zaid Siddiquee K and Turkson J: STAT3 as a target for inducing apoptosis in solid and hematological tumors. Cell Res 18: 254-267, 2008.
26. Barry SP, Townsend PA, Knight RA, Scarabelli TM, Latchman DS and Stephanou A: STAT3 modulates the DNA damage response pathway. Int J Exp Pathol 91: 506-514, 2010.
27. Koganti S, Hui-Yuen J, McAllister S, Gardner B, Grasser F, Palendira U, Tangye SG, Freeman AF and Bhaduri-McIntosh S: STAT3 interrupts ATR-Chk1 signaling to allow oncovirus-mediated cell proliferation. Proc Natl Acad Sci USA 111: 4946-4951, 2014.

28. Deng WW, Hu Q, Liu ZR, Chen QH, Wang WX, Zhang HG, Zhang Q, Huang YL and Zhang XK: KDM4B promotes DNA damage response via STAT3 signaling and is a target of CREB in colorectal cancer cells. Mol Cell Biochem 449: 81-90, 2018.
29. De Groef S, Renmans D, Cai Y, Leuckx G, Roels S, Staels W, Gradwohl G, Baeyens L, Heremans Y, Martens GA, *et al*: STAT3 modulates β-cell cycling in injured mouse pancreas and protects against DNA damage. Cell Death Dis 7: e2272, 2016.
30. Yu H, Pardoll D and Jove R: STATs in cancer inflammation and immunity: A leading role for STAT3. Nat Rev Cancer 9: 798-809, 2009.